HHS Public Access

Author manuscript

J Micromech Microeng. Author manuscript; available in PMC 2019 February 01.

Published in final edited form as:

J Micromech Microeng. 2018 February ; 28(2): . doi:10.1088/1361-6439/aaa0ae.

Acoustic Actuation of *in situ* Fabricated Artificial Cilia

Sinem Orbay[1,*], **Adem Ozcelik**[2,*], **Hunter Bachman**[3], and **Tony Jun Huang**[3]

[1]Institute of Biomedical Engineering, Bogazici University, Cengelkoy, Istanbul, 34684, Turkey

[2]Department of Electronics and Automation, Soma Vocational School, Manisa Celal Bayar University, Soma, Manisa, 45500, Turkey

[3]Department of Mechanical Engineering and Material Science, Duke University, Durham, NC, 27708, USA

Abstract

We present on-chip acoustic actuation of *in situ* fabricated artificial cilia. Arrays of cilia structures are UV polymerized inside a microfluidic channel using a photocurable polyethylene glycol (PEG) polymer solution and photomasks. During polymerization, cilia structures are attached to a silane treated glass surface inside the microchannel. Then, the cilia structures are actuated using acoustic vibrations at 4.6 kHz generated by piezo transducers. As a demonstration of a practical application, DI water and fluorescein dye solutions are mixed inside a microfluidic channel. Using pulses of acoustic excitations, and locally fabricated cilia structures within a certain region of the microchannel, a waveform of mixing behavior is obtained. This result illustrates one potential application wherein researchers can achieve spatiotemporal control of biological microenvironments in cell stimulation studies. These acoustically actuated, *in situ* fabricated, cilia structures can be used in many on-chip applications in biological, chemical and engineering studies.

Keywords

Artificial cilia; micromixing; acoustofluidics; microfluidics

1. Introduction

Motile cilia are fundamental cellular tools used to manipulate fluid flow in many biological systems including kidneys, respiratory systems, sperms, and oviducts [1,2]. For example, cilia covering respiratory tracts help keep the airways free of dirt and mucus, and cilia on ependymal cells in the ventricles of the brain provide circulation of cerebrospinal fluid throughout the ventricular system [3]. The fluid handling capability of motile cilia is derived from their rhythmic beating motions that also distinguish them from nonmotile primary cilia [4]. If fabrication and actuation of artificial cilia that is inspired from the biological counterparts can be simple and efficient, on-chip regulation of fluidic environment locally

*Equal contribution

and globally can facilitate critical lab-on-a-chip functions such as fluid mixing, pumping, and spatiotemporal control of biochemical microenvironments [5].

Within the last decade, there have been many demonstrations of the fabrication and actuation of artificial cilia in order to achieve various lab-on-a-chip functions, such as directional fluid transport, fluid mixing, regulating material deposition, organism alignment, sperm cell activation, and mobile microrobots [6–14]. Polydimethylsiloxane (PDMS) has been widely used to fabricate cilia through the replica molding technique [15–18]. Yang *et al.* studied fabrication parameters of passive PDMS cilia arrays for applications in measuring cell traction forces [19]. PDMS cilia fabrication via this approach requires multi-step photolithography and replica molding in a cleanroom microfabrication facility that is not readily available to most research labs in developing countries. Wang *et al.* introduced the continuous roll-pulling technique to fabricate PDMS cilia through pulling filaments from a liquid PDMS layer, and subsequently curing them in an oven to obtain soft artificial cilia [20]. This method is useful for eliminating expensive cleanroom fabrication steps, but is limited by the pillar geometry of the roller and lacks dynamic spatial control of the fabricated cilia location. While each of these previous fabrication methods demonstrated unique solutions for molding artificial cilia, there remains room for advancement to a simpler, more efficient, and more tunable fabrication method.

Actuation of artificial cilia by using magnetic fields has been demonstrated by many researchers; this method requires mixing and dispersing magnetic particles inside the soft polymeric network of the cilia material before curing [21–25]. Lee *et al.* computationally analyzed the resonant behavior of artificial cilia due to an added mass effect that may be insightful for designing new artificial cilia applications [26]. Additionally, several methods for fabricating these magnetic based cilia do not depend on magnetizing PDMS or using the elastomer to encapsulate a magnetic material [27,28]. In such methods, specialized magnetic materials form into cilia via self-assembly. These materials are highly functionalized and can closely mimic natural cilia motion without the need for an elastomeric binder. Chemically induced cilia oscillation using the Belousov–Zhabotinsky reaction was also computationally demonstrated, but application of this method in lab-on-a-chip microfluidic platforms may not be feasible due to the required medium properties and limited supply of reaction chemicals [29]. Based on the existing literature surrounding artificial cilia, there is a need for a simple fabrication method and straightforward actuation technique for artificial cilia to be adapted by the lab-on-a-chip community.

In this work, we present a new approach to artificial cilia fabrication and actuation using soft hydrogel polymers and acoustic waves, respectively. In particular, we use photocrosslinkable polyethylene (glycol) diacrylate (PEGDA) polymers to fabricate artificial cilia directly inside a microfluidic channel; the cilia fixed to a glass substrate from one end and free at the other. Then, we use acoustofluidics [30–36], the fusion of acoustics and microfluidics, to drive these cilia structures inside a microchannel to perform fluid actuation. Owing to their simple fabrication and easy actuation, acoustically driven artificial cilia hold great promise for various lab-on-a-chip applications in chemical, biological, and engineering sciences.

2. Method

To fabricate the microfluidic channels, photolithography and replica molding methods were used. Briefly, a 4-inch silicon wafer coated with hexamethyldisilazane (HMDS) was spin-casted and patterned with a positive photoresist (Megaposit SPR955, Microchem, USA). Then, the silicon master mold was fabricated through deep reactive ion etching (DRIE) using an Alcatel Speeder 100Si BOSCH etch system. After cleaning the surface of the etched wafer with copious amount of acetone (97065-060, VWR, USA), it was treated with chlorotrimethylsilane vapor (75-77-4, Alfa Aesar, USA) to help in the mold releasing process. Then, a 10:1 ratio of PDMS resin and curing agent (Sylgard 184, Dow-Corning, USA) was mixed, degassed, and poured onto the chlorotrimethylsilane vapor treated master mold, and subsequently cured at 65 °C for two hours. PDMS microchannels with width, depth, and length of 250 μm, 175 μm, and 1.2 mm, respectively, were released, and their inlets and outlets were formed using a biopsy punch (Harris Uni-Core 0.75 mm, USA). Individual microchannels and glass slides (48404-454, VWR, USA) were plasma treated and attached together using a high-frequency generator (BD-10AS, Electro-Technic Products, USA), and baked at 65 °C overnight to promote strong bonding. A piezoelectric transducer (81-7BB-27-4L0, Murata Electronics, Japan) was bonded next to the PDMS microchannel using a thin layer of epoxy (G14250, Devcon, USA). Polyethylene tubes (10793527, Smith's Medical, USA) were inserted into the inlets and outlet of the PDMS device.

For cilia fabrication, we used a solution of 40% (v/v) polyethylene glycol (PEG) diacrylate with a molecular weight of 700 (PEG700, Sigma-Aldrich, USA), 30% (v/v) PEG with a molecular weight of 258 (PEG 258, Sigma-Aldrich, USA), 15% (v/v) photo-initiator 2-Hydroxy-2-methyl-1-phenyl-propan-1-one (Darocur 1173, Ciba, USA), and 15% (v/v) TE buffer (100 TE, OmniPur, USA) [37,38]. To UV polymerize this solution, we used an inverted Nikon microscope (TE-2000U, Nikon, Japan) equipped with 10X objective lens (Plan Fluor 10x/0.3 DIC L/N1, infinity/0.17 WD 16.0, Nikon, Japan), a filter cube (11000v3: UV, Chroma), and a mercury lamp (Intensilight C-HGFI, Nikon, Japan). A photomask with an array of transparent holes was used to obtain base patterns of the cilia arrays (Figure 1). The UV exposure time of 100 ms was controlled by a computer-controlled mechanical shutter (LB-SC, Sutter Instrument Company, USA). Once the polymer solution was injected inside the PDMS device, UV light was used to expose and polymerize the solution and form an array of cilia (Figure 1). These polymerized cilia structures reached from the glass slide surface to the ceiling of the microchannel leaving a thin (1–3 μm) oxygen inhibition layer at the top of the microchannel owing to the oxygen permeable feature of PDMS [39]. The glass slide surface inside the PDMS channel was previously treated with chlorotrimethylsilane vapor under vacuum to improve the polymer attachment to the glass slide during UV polymerization. After cilia fabrication, the microchannel was flushed with ethanol to remove the unpolymerized polymer solution, revealing an array of artificial cilium structures only attached to the glass surface. To actuate the fabricated cilia structures, the piezoelectric transducer (PZT) was driven by sine-wave signals from a function generator (AFG3011, Tektronix, USA), and amplified by an RF amplifier (25A250A, Amplifier Research, USA). For mixing demonstrations, DI water and fluorescein

dye (F7250, Sigma-Aldrich, USA) solutions were infused inside the microchannel using a syringe pump (neMESYS, Germany) at a total flow rate of 5 μl/min.

3. Results and Discussion

We aimed to fabricate soft, artificial cilia arrays to be activated externally in microfluidic channels. The photomask with 300 μm transparent holes inserted to the field stop of the microscope with 10x objective lens and 100 ms UV exposure time yielded about 30 μm average diameter cilia structures (Figure 2). By changing the design of the photomask, cilia geometry could be easily modified as well (Figure 2(b)). The height of the cilia was measured to be ~170 μm, which was determined by the channel height and the oxygen inhibition layer in our PDMS channels. The UV cured polymers in this work is expected to have an elastic modulus between 100 kPa and 500 kPa based on the reported mechanical properties of the similar polymer hydrogels [40]. As a comparison, the 1:10 ratio PDMS structure that was used for the microfluidic channel material has an elastic modulus around 2.6 MPa [41]. To minimize the elastic modulus and geometry variations among the cilia structures due to UV light intensity change across the beam diameter, we used photomasks with only a few rows of cilia at the center of the mask. Larger arrays of cilia were fabricated by shifting the microfluidic channel and repeating the UV fabrication step. Potentially, using a digital micromirror device (DMD), the diameter, geometry, and spacing of cilia arrays could be tuned dynamically. The simplicity of fabricating the cilia structures inside an existing microchannel provides a practical approach compared to traditional cilia fabrication techniques, such that any number of cilia can be added to any desired position of a microfluidic device for additional functions and complexity. Furthermore, the composition of the polymer solution can be chosen to add even more functionalities such as magnetic particles for magnetic attraction, biological reagents for sensing, or catalytic particles for catalyzing reactions in microfluidic syntheses [28,42–46].

We actuated the cilia structures with the highest amount of deflection by driving the bonded piezo transducer at its resonance frequency which was ~ 4.6 kHz (Figures 3(a)–(b) and Supplementary Movie 1). By applying increasing voltages to the transducer from 20 to 140 V_{PP} (volt peak-to-peak), the deflection amount of the cilia structures increased (Figure 3(d)). The deflection amount, which was measured as the maximum distance of a point on the top of a cilium during one cycle of oscillation, was found to be linearly increasing with the increasing driving voltage. The direction of the cilia oscillation was found to be independent of the relative position of the transducer with respect to the microchannel. That is, the cilia structures performed the same horizontal movement as shown in Figure 3(a), when actuated at the same driving frequency, regardless of whether the transducer was placed in front of or next to the PDMS channel. We believe that the oscillation direction is determined by the oscillation of the glass coverslip that the cilia are attached to. As such, the oscillation direction of the cilia is predetermined by the wave pattern on the glass substrate. Supporting this conclusion, by tuning the frequency, slightly different cilia oscillation directions were observed, but the deflection amount for such cases were much lower. We targeted the maximum cilia deflection amount, which generally happened at the resonance frequency of ~4.6 kHz. Additional parameters that affect the cilia deflection magnitude include the height and diameter of the structures, but these features were kept constant in this study. As the

channel height increases or cilia dimeter decreases, we would expect the deflection amount to increase according to the linear theory of elasticity [47].

Even though microfluidics provides many advantages [48–51], fluid mixing is still one of the biggest challenges due to low Reynolds numbers and slow mixing time [52–54]. To demonstrate the fluid manipulation capabilities of acoustically actuated artificial cilia structures, we first used a mixing example (Figure 4). In the absence of an acoustic field, DI water and fluorescein dye solutions flow side-by-side in a laminar flow regime without significant mixing at a total flow rate of 5 μl/min. Once the transducer was turned on, actuation of the cilia array completely mixed the two fluids as shown in Figure 4(b). The mixing mechanism of artificial cilia structures have been studied in terms of Sperm number (S_p) that characterized the secondary flows generated due to coupling between elastic cilium bending and viscous fluid forces [4,55–58]. S_p is a dimensionless number and is given by [56];

$$S_p = L\left(\frac{4\pi\mu\omega}{EI}\right)^{1/4} \quad (1)$$

where L, μ, ω, E and I are length of the cilia, dynamic viscosity of the fluid medium, angular velocity of the cilia oscillation, elastic modulus, and moment of inertia of the cilia. For 170 μm long, and 30 μm diameter cilia structures oscillating at 4.6 kHz in water, S_p ranges from 1.5 to 1 for 100 kPa and 500 kPa elastic modulus values, respectively. In our experimental setup, the oscillation frequency of the cilia is determined by the resonance condition of the transducer and the glass slide such that even 5% deviation from the resonant frequency greatly reduced the oscillation amplitude of the cilia. If we could oscillate these cilia structures at lower frequencies such as 100 Hz using transducers and base substrates with lower working frequencies, S_p would vary from 0.5 to 0.3 for the same range of elastic modulus values. For larger S_p values, viscous forces dominate and reduce the net fluid flow eventually to zero. For smaller S_p values elasticity dominates which lead to time-reversible cilia oscillation that cannot generate net fluid flow. For an intermediate S_p value fluid displacement reaches to a maximum [4,56,59]. In our case, S_p falls roughly into the intermediate region. With longer cilia structures or higher oscillation frequencies, S_p could be increased slightly.

Even though the Reynolds number of the fluid flow in the absence of the cilia oscillation is less than 0.1, the strong nonlinear effects due to cilia oscillations indicate that the local Reynolds number should not be as low [38]. Reynolds number is given by UR/ν where U, R, and ν are characteristic speed, characteristic length, and kinematic viscosity, respectively. Using 50 micrometers as the deflection magnitude for a cilium, the speed of the tip of the cilium can be estimated as 2.3×10^5 μm s^{-1} for the oscillation frequency of 4.6 kHz. The diameter of the cilium is around 30 μm, and the kinematic viscosity of DI water is around 1×10^6 $(\mu m)^2$ s^{-1}. Reynolds number that is corresponding to this motion is found approximately 7. Normalized gray scale intensity plot along the two dotted lines shown in Figure 4(a) and (b) quantitatively shows mixing of two fluids before and after the cilia field

(Supplementary Movie 2). To evaluate the mixing quality, we used the mixing index given by [60];

$$M = 1 - \sqrt{\frac{1/n\sum((I_i - I_m)^2}{I_m}} \quad (2)$$

where M is the mixing index, n is the total number of points, I_i is the intensity of each point, and I_m is the average intensity. For unmixed flows M becomes 0, and for completely mixed fluids M becomes 1. A mixing index value of 0.9 or higher indicates homogenous mixing [61]. In our application, mixing index was found to be ~0.92 which indicates good mixing behavior. We believe that the mixing performance could be improved by modifying the cilia's geometric parameters to increase their deflection (i.e. decrease cilia diameter or increase cilia height). Further study is needed to investigate this hypothesis

In addition to continuous uniform fluid mixing, we also demonstrated on-demand and pulsatile local mixing using a smaller number of cilia (Figure 5). In this example, a region of interest (ROI) was selected between two cilia structures as shown in Figure 5(a) and (b). Before the actuation of the cilia structures, the ROI overlapped with the DI water flow region that appeared as dark under the fluorescent microscope. Upon application of a short pulse of acoustic excitation, the ROI overlapped with the mixed fluids that appeared as a bright field. By repeating the acoustic pulses, a wave form of grayscale intensity values inside the ROI was obtained (Figure 5(c) and Supplementary Movie 3). This graph resembles a chemical waveform in a local microenvironment. By using our acoustically driven artificial cilia structures in different numbers and at selected positions, it is possible to change chemical environments of on-chip cultured cells in order to study effects of different concentrations and exposure times of chemical stimulations on cell biology. More specifically, rapid chemical waveform generation has been demonstrated as a useful tool for investigating both cellular response as well as subcellular pathways, which are crucial to understanding cell migration and adaptation for inflammatory response or cancer metastasis [32,62,63].

4. Conclusions

We demonstrated on-chip acoustic actuation of *in situ* fabricated artificial cilia. The cilia structures were driven into oscillatory motion using a 4.6 kHz frequency and 20 to 140 V_{PP} amplitude sine wave. The deflection magnitude of the cilia was found to increase linearly with the voltage up to a maximum of 55 μm, which was sufficient to mix DI water and fluorescein solutions in the microfluidic channel. Using pulses of acoustic excitation, a waveform-like mixing behavior was also obtained. The cilia fabrication approach presented here provides several advantages over traditional techniques, such as simple formation and geometric adaptability, and also removes the need for a cleanroom to fabricate the cilia beyond the initial photolithography process for microchannel mold fabrication. Acoustic actuation of the cilia structures also has advantages over magnetic methods because there is no need for the cilia to be magnetized, a requirement that adds more steps to the fabrication

process. Additionally, compared to more complex magnetic field generation setups, acoustic field generation is provided by a simple piezo transducer that can be purchased for less than $1. The ability to mix fluids locally and on-demand can potentially be used in on-chip cell stimulation studies where spatiotemporal control of various chemicals is needed. Combining simple fabrication and convenient actuation, our *in situ* fabricated, acoustically actuated artificial cilia structures can be used in many lab-on-a-chip and organ-on-chip applications.

Supplementary Material

Refer to Web version on PubMed Central for supplementary material.

Acknowledgments

The authors acknowledge support from the National Institutes of Health (R01 GM112048 and R33 EB019785) and the National Science Foundation (IDBR-1455658 and IIP-1534645). Components of this work were conducted at the Penn State node of the NSF-funded National Nanotechnology Infrastructure Network.

References

1. Mitchison HM, Valente EM. Motile and non-motile cilia in human pathology: from function to phenotypes. J Pathol. 2017; 241:294–309. [PubMed: 27859258]
2. Ostrowski LE, Dutcher SK, Lo CW. Cilia and Models for Studying Structure and Function. Proc Am Thorac Soc. 2011; 8:423–9. [PubMed: 21926393]
3. Nawroth JC, Guo H, Koch E, Heath-Heckman EAC, Hermanson JC, Ruby EG, Dabiri JO, Kanso E, McFall-Ngai M. Motile cilia create fluid-mechanical microhabitats for the active recruitment of the host microbiome. Proc Natl Acad Sci. 2017; 114:9510–6. [PubMed: 28835539]
4. Masoud H, Alexeev A. Harnessing synthetic cilia to regulate motion of microparticles. Soft Matter. 2011; 7:8702.
5. Nge PN, Rogers CI, Woolley AT. Advances in Microfluidic Materials, Functions, Integration, and Applications. Chem Rev. 2013; 113:2550–83. [PubMed: 23410114]
6. Khaderi SN, Craus CB, Hussong J, Schorr N, Belardi J, Westerweel J, Prucker O, Rühe J, den Toonder JMJ, Onck PR. Magnetically-actuated artificial cilia for microfluidic propulsion. Lab Chip. 2011; 11:2002. [PubMed: 21331419]
7. Sing CE, Schmid L, Schneider MF, Franke T, Alexander-Katz A. Controlled surface-induced flows from the motion of self-assembled colloidal walkers. Proc Natl Acad Sci. 2010; 107:535–40. [PubMed: 20080716]
8. den Toonder JMJ, Onck PR. Microfluidic manipulation with artificial/bioinspired cilia. Trends Biotechnol. 2013; 31:85–91. [PubMed: 23245658]
9. Chen C-Y, Chang Chien T-C, Mani K, Tsai H-Y. Axial orientation control of zebrafish larvae using artificial cilia. Microfluid Nanofluidics. 2016; 20:12.
10. den Toonder J, Bos F, Broer D, Filippini L, Gillies M, de Goede J, Mol T, Reijme M, Talen W, Wilderbeek H, Khatavkar V, Anderson P. Artificial cilia for active micro-fluidic mixing. Lab Chip. 2008; 8:533. [PubMed: 18369507]
11. Huang P-Y, Panigrahi B, Lu C-H, Huang P-F, Chen C-Y. An artificial cilia-based micromixer towards the activation of zebrafish sperms. Sensors Actuators B Chem. 2017; 244:541–8.
12. Branscomb J, Alexeev A. Designing ciliated surfaces that regulate deposition of solid particles. Soft Matter. 2010; 6:4066.
13. Shields aRFiser BL, Evans BaFalvo MR, Washburn S, Superfine R. Biomimetic cilia arrays generate simultaneous pumping and mixing regimes. Proc Natl Acad Sci. 2010; 107:15670–5. [PubMed: 20798342]
14. Sareh S, Rossiter J, Conn A, Drescher K, Goldstein RE. Swimming like algae: biomimetic soft artificial cilia. J R Soc Interface. 2012; 10:20120666–20120666. [PubMed: 23097503]

15. Mills ZG, Aziz B, Alexeev A. Beating synthetic cilia enhance heat transport in microfluidic channels. Soft Matter. 2012; 8:11508.
16. Bhattacharya A, Balazs AC. Stiffness-modulated motion of soft microscopic particles over active adhesive cilia. Soft Matter. 2013; 9:3945.
17. Oh K, Chung J-H, Devasia S, Riley JJ. Bio-mimetic silicone cilia for microfluidic manipulation. Lab Chip. 2009; 9:1561. [PubMed: 19458863]
18. Evans BaShields aRCarroll RL, Washburn S, Falvo MR, Superfine R. Magnetically Actuated Nanorod Arrays as Biomimetic Cilia. Nano Lett. 2007; 7:1428–34. [PubMed: 17419660]
19. Yang MT, Sniadecki NJ, Chen CS. Geometric Considerations of Micro- to Nanoscale Elastomeric Post Arrays to Study Cellular Traction Forces. Adv Mater. 2007; 19:3119–23.
20. Wang Y, den Toonder J, Cardinaels R, Anderson P. A continuous roll-pulling approach for the fabrication of magnetic artificial cilia with microfluidic pumping capability. Lab Chip. 2016; 16:2277–86. [PubMed: 27210071]
21. Fahrni F, Prins MWJ, van IJzendoorn LJ. Micro-fluidic actuation using magnetic artificial cilia. Lab Chip. 2009; 9:3413. [PubMed: 19904409]
22. Liu F, Zhang J, Alici G, Yan S, Mutlu R, Li W, Yan T. An inverted micro-mixer based on a magnetically-actuated cilium made of Fe doped PDMS. Smart Mater Struct. 2016; 25:95049.
23. Liu F, Alici G, Zhang B, Beirne S, Li W. Fabrication and characterization of a magnetic micro-actuator based on deformable Fe-doped PDMS artificial cilium using 3D printing. Smart Mater Struct. 2015; 24:35015.
24. Gauger EM, Downton MT, Stark H. Fluid transport at low Reynolds number with magnetically actuated artificial cilia. Eur Phys J E. 2009; 28:231–42. [PubMed: 19030903]
25. Wu Y-A, Panigrahi B, Chen C-Y. Hydrodynamically efficient micropropulsion through a new artificial cilia beating concept. Microsyst Technol. 2017
26. Lee T-R, Oh K, Chung J-H, Chang Y-S, Choi J-B, Yagawa G, Kim Y-J. Resonant behavior and microfluidic manipulation of silicone cilia due to an added mass effect. Soft Matter. 2011; 7:4325.
27. Vilfan M, Potocnik A, Kavcic B, Osterman N, Poberaj I, Vilfan A, Babic D. Self-assembled artificial cilia. Proc Natl Acad Sci. 2010; 107:1844–7. [PubMed: 19934055]
28. Li C, Lo C-W, Zhu D, Li C, Liu Y, Jiang H. Synthesis of a Photoresponsive Liquid-Crystalline Polymer Containing Azobenzene. Macromol Rapid Commun. 2009; 30:1928–35. [PubMed: 21638477]
29. Dayal P, Kuksenok O, Bhattacharya A, Balazs AC. Chemically-mediated communication in self-oscillating, biomimetic cilia. J Mater Chem. 2012; 22:241–50.
30. Ayan B, Ozcelik A, Bachman H, Tang S-Y, Xie Y, Wu M, Li P, Huang TJ. Acoustofluidic coating of particles and cells. Lab Chip. 2016; 16:4366–72. [PubMed: 27754503]
31. Ozcelik A, Nama N, Huang P-H, Kaynak M, McReynolds MR, Hanna-Rose W, Huang TJ. Acoustofluidic Rotational Manipulation of Cells and Organisms Using Oscillating Solid Structures. Small. 2016; 12:5230–5230.
32. Ahmed D, Muddana HS, Lu M, French JB, Ozcelik A, Fang Y, Butler PJ, Benkovic SJ, Manz A, Huang TJ. Acoustofluidic Chemical Waveform Generator and Switch. Anal Chem. 2014; 86:11803–10. [PubMed: 25405550]
33. Ahmed D, Peng X, Ozcelik A, Zheng Y, Huang TJ. Acousto-plasmofluidics: Acoustic modulation of surface plasmon resonance in microfluidic systems. AIP Adv. 2015; 5:97161.
34. Nawaz AA, Chen Y, Nama N, Nissly RH, Ren L, Ozcelik A, Wang L, McCoy JP, Levine SJ, Huang TJ. Acoustofluidic Fluorescence Activated Cell Sorter. Anal Chem. 2015; 87:12051–8. [PubMed: 26331909]
35. Ozcelik A, Ahmed D, Xie Y, Nama N, Qu Z, Nawaz AA, Huang TJ. An Acoustofluidic Micromixer via Bubble Inception and Cavitation from Microchannel Sidewalls. Anal Chem. 2014; 86:5083–8. [PubMed: 24754496]
36. Orbay S, Ozcelik A, Lata J, Kaynak M, Wu M, Huang TJ. Mixing high-viscosity fluids via acoustically driven bubbles. J Micromechanics Microengineering. 2017; 27:15008.
37. Kaynak M, Ozcelik A, Nourhani A, Lammert PE, Crespi VH, Huang TJ. Acoustic actuation of bioinspired microswimmers. Lab Chip. 2017; 17:395–400. [PubMed: 27991641]

38. Kaynak M, Ozcelik A, Nama N, Nourhani A, Lammert PE, Crespi VH, Huang TJ. Acoustofluidic actuation of in situ fabricated microrotors. Lab Chip. 2016; 16:3532–7. [PubMed: 27466140]
39. Dendukuri D, Pregibon DC, Collins J, Hatton TA, Doyle PS. Continuous-flow lithography for high-throughput microparticle synthesis. Nat Mater. 2006; 5:365–9. [PubMed: 16604080]
40. Yang Ting. Mechanical and Swelling Properties of Hydrogels. Royal Institute of Technology; Sweden: 2012.
41. Wang Z. Polydimethylsiloxane Mechanical Properties Measured by Macroscopic Compression and Nanoindentation Technique. University of Florida; USA: 2011.
42. Liu Y, Cheng D, Lin I-H, Abbott NL, Jiang H. Microfluidic sensing devices employing in situ-formed liquid crystal thin film for detection of biochemical interactions. Lab Chip. 2012; 12:3746. [PubMed: 22842797]
43. Lee H, Xu L, Koh D, Nyayapathi N, Oh K. Various On-Chip Sensors with Microfluidics for Biological Applications. Sensors. 2014; 14:17008–36. [PubMed: 25222033]
44. Xu L, Lee H, Panchapakesan R, Oh KW. Fusion and sorting of two parallel trains of droplets using a railroad-like channel network and guiding tracks. Lab Chip. 2012; 12:3936. [PubMed: 22814673]
45. Liu X, Lillehoj PB. Embroidered electrochemical sensors on gauze for rapid quantification of wound biomarkers. Biosens Bioelectron. 2017; 98:189–94. [PubMed: 28675839]
46. Lillehoj PB, Huang M-C, Truong N, Ho C-M. Rapid electrochemical detection on a mobile phone. Lab Chip. 2013; 13:2950. [PubMed: 23689554]
47. Gurtin ME. The Linear Theory of Elasticity. In: Truesdell C, editorLinear Theories of Elasticity and Thermoelasticity. Berlin, Heidelberg: Springer Berlin Heidelberg; 1973. 1–295.
48. Hung L-Y, Wu H-W, Hsieh K, Lee G-B. Microfluidic platforms for discovery and detection of molecular biomarkers. Microfluid Nanofluidics. 2014; 16:941–63.
49. Hung L-Y, Chuang Y-H, Kuo H-T, Wang C-H, Hsu K-F, Chou C-Y, Lee G-B. An integrated microfluidic platform for rapid tumor cell isolation, counting and molecular diagnosis. Biomed Microdevices. 2013; 15:339–52. [PubMed: 23315192]
50. Que L, Wilson CG, Gianchandani YB. Microfluidic electrodischarge devices with integrated dispersion optics for spectral analysis of water impurities. J Microelectromechanical Syst. 2005; 14:185–91.
51. Basu AS, Gianchandani YB. Virtual microfluidic traps, filters, channels and pumps using Marangoni flows. J Micromechanics Microengineering. 2008; 18:115031.
52. Ballard M, Owen D, Mills ZG, Hesketh PJ, Alexeev A. Orbiting magnetic microbeads enable rapid microfluidic mixing. Microfluid Nanofluidics. 2016; 20:88.
53. Coleman JT, Sinton D. A sequential injection microfluidic mixing strategy. Microfluid Nanofluidics. 2005; 1:319–27.
54. Coleman JT, McKechnie J, Sinton D. High-efficiency electrokinetic micromixing through symmetric sequential injection and expansion. Lab Chip. 2006; 6:1033. [PubMed: 16874374]
55. Wiggins CH, Riveline D, Ott A, Goldstein RE. Trapping and Wiggling: Elastohydrodynamics of Driven Microfilaments. Biophys J. 1998; 74:1043–60. [PubMed: 9533717]
56. Lowe CP. Dynamics of filaments: modelling the dynamics of driven microfilaments. Philos Trans R Soc B Biol Sci. 2003; 358:1543–50.
57. Ghosh R, Buxton GA, Usta OB, Balazs AC, Alexeev A. Designing Oscillating Cilia That Capture or Release Microscopic Particles. Langmuir. 2010; 26:2963–8. [PubMed: 19799457]
58. Alexeev A, Yeomans JM, Balazs AC. Designing Synthetic, Pumping Cilia That Switch the Flow Direction in Microchannels. Langmuir. 2008; 24:12102–6. [PubMed: 18847292]
59. Alexeev A, Ghosh R, Buxton GA, Usta OB, Balazs AC. Using Actuated Cilia to Regulate Motion of Microscopic Particles. ASME 2010 First Global Congress on NanoEngineering for Medicine and Biology; ASME; 2010. 43–4.
60. Li Y, Xu Y, Feng X, Liu B. A rapid microfluidic mixer for high-viscosity fluids to track ultrafast early folding kinetics of G-quadruplex under molecular crowding conditions. Anal Chem. 2012; 84:9025–32. [PubMed: 23020167]

61. Hashmi A, Xu J. On the Quantification of Mixing in Microfluidics. J Lab Autom. 2014; 19:488–91. [PubMed: 24963095]

62. Meier B, Zielinski A, Weber C, Arcizet D, Youssef S, Franosch T, Radler JO, Heinrich D, Rädler JO, Heinrich D. Chemotactic cell trapping in controlled alternating gradient fields. Proc Natl Acad Sci. 2011; 108:11417–22. [PubMed: 21709255]

63. Hersen P, McClean MN, Mahadevan L, Ramanathan S. Signal processing by the HOG MAP kinase pathway. Proc Natl Acad Sci. 2008; 105:7165–70. [PubMed: 18480263]

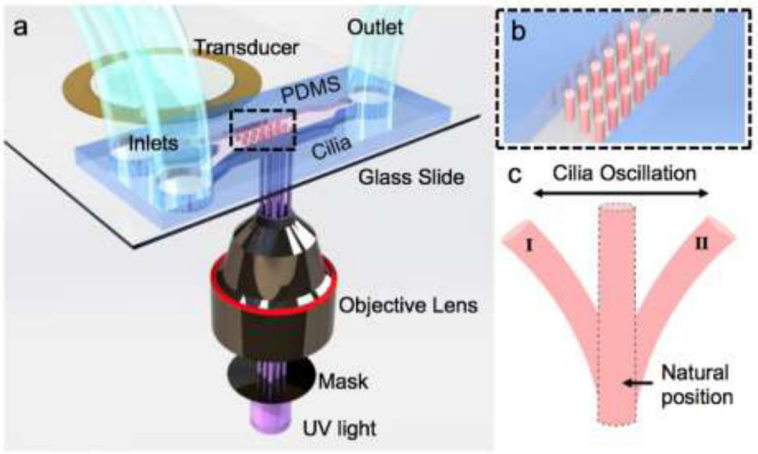

Figure 1.

Schematic depiction of artificial cilia fabrication and actuation (not to scale). (a) An assembly of a microfluidic channel and a piezoelectric transducer is placed within the optical path of an inverted microscope. (b) An array of UV fabricated cilia inside the channel is illustrated in close view. (c) Depiction of the anticipated cilia motion during acoustic excitations.

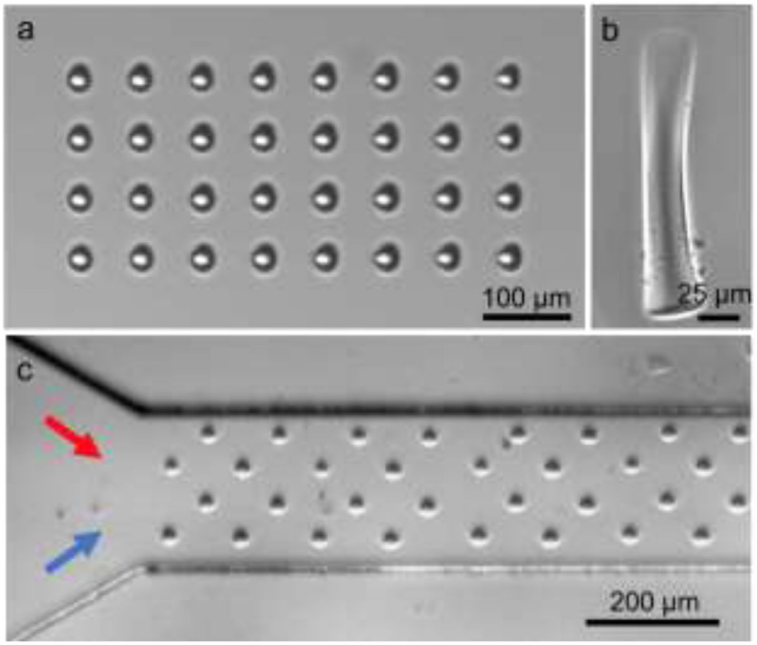

Figure 2.

Optical images of artificial cilia structures. (a) Top view of the fabricated cilia structures in the microfluidic channel. (b) Side view of a single cilium. (c) Top view of a two inlet channel with a repeated pattern of cilia structures. The red and blue arrows represent two fluids to be injected inside the channel.

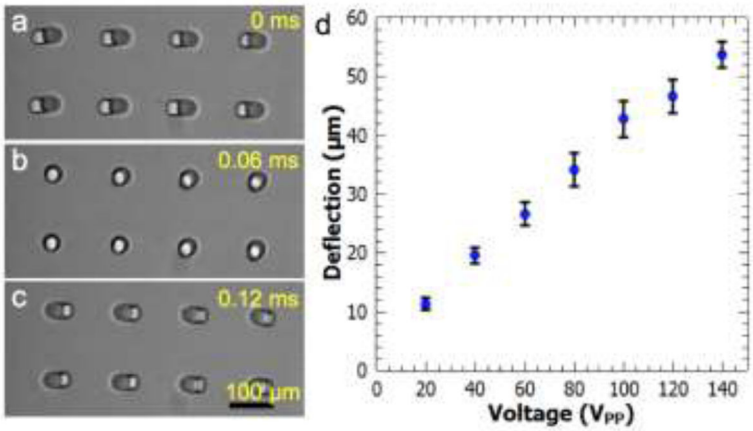

Figure 3.

Acoustic actuation of cilia structures. (a)–(c) An array of 8 cilium structures oscillates left-to-right under constant acoustic excitation. (d) Deflection distance is plotted as a function of the applied voltage to the transducer at the fixed frequency of 4.6 kHz. Error bars represent standard deviation of at least 6 different measurements.

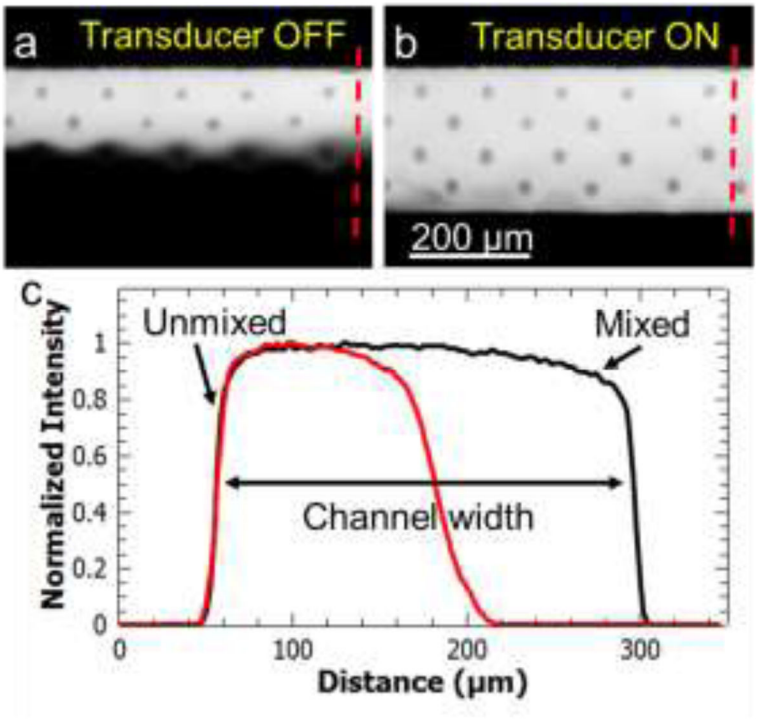

Figure 4.

Mixing demonstration using acoustically driven cilia. (a) DI water and fluorescein dye flows side by side without any significant mixing in the absence of cilia actuation. (b) When the piezoelectric transducer is turned on, two solutions are mixed in ~100 milliseconds by the actuation of cilia structures. (c) Intensity plot (normalized to 1) along the dotted lines in (a) and (b) shows homogenous mixing that is characterized with a mixing index of ~0.92.

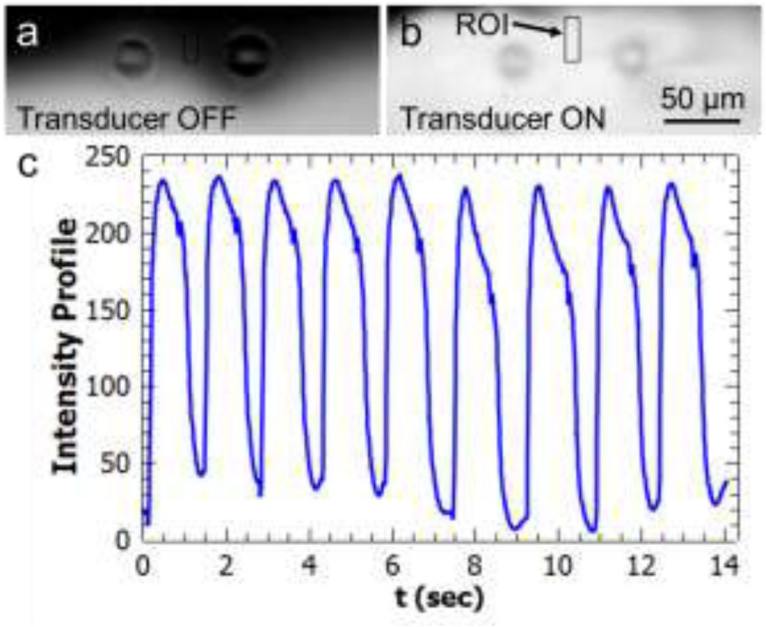

Figure 5.

Pulsatile, on-demand mixing demonstration using two cilia structures by DI water and fluorescein dye solutions. (a) A region of interest (ROI) is determined between two cilia structures. The ROI is dark when the transducer is off. (b) By application of a pulse of acoustic excitation, the DI water and fluorescein solutions are mixed and the ROI becomes bright. (c) Periodically applied acoustic excitations generate pulses of fluid mixing resembling a chemical waveform.